

PHOTOINJECTORS R&D FOR FUTURE LIGHT SOURCES & LINEAR COLLIDERS*

P. Piot, Northern Illinois University, DeKalb, IL 60115, USA
Fermi National Accelerator Laboratory, Batavia, IL 60510, USA

Abstract

Linac-driven light sources and proposed linear colliders require high brightness electron beams. In addition to the small emittances and high peak currents, linear colliders also require spin-polarization and possibly the generation of asymmetric beam in the two transverse degrees of freedom. Other applications (e.g., high-average-power free-electron lasers) call for high duty cycle and/or (e.g., electron cooling) angular-momentum-dominated electron beams. We review ongoing R&D programs aiming at the production of electron beams satisfying these various requirements. We especially discuss R&D on photoemission electron sources (with focus on radiofrequency guns) along with the possible use of emittance-manipulation techniques.

INTRODUCTION

Photoemission offers significant advantages over other popular emission processes (e.g., thermionic emission). In principle one has good control over the initial transverse and longitudinal distributions of the emitted electron bunch by properly shaping the photocathode-drive-laser pulse. This feature of photoemission sources turn out to be a key factor in optimizing the beam parameters. The availability of short laser pulses enables production of electron bunches with length shorter than the radiofrequency (rf) wavelength. Therefore, a photoinjector circumvents the bunching schemes (chopper and sub-harmonic bunchers) needed in other types of injectors. Photoemission can provide charge densities that are two orders of magnitude higher than thermionic emission. Finally a circularly polarized laser impinging a suitable photocathode enables the production of spin-polarized electrons. Because of the high charge density, the photoelectrons need to be accelerated as promptly as possible to avoid significant space-charge-induced dilution of their phase space. Hence the photocathode is either located on the back plate of the half-cell of a resonant rf cavity (rf gun) or at an extremity of a high-voltage gap (dc gun).

Photoinjectors [1] are popular electron sources that have been subject to intense research over the past years and are now used in operating accelerators. Their applications range from high-energy physics (e.g., electron source for colliders, electron cooling) to light sources [e.g., single-

pass, high-gain free-electron lasers (FELs)].

The figure-of-merit depends upon the front-end application, but typically the phase-space density associated with a single bunch needs to be maximized. A widely accepted parameter to compare electron sources is the single-bunch brightness defined as

$$\mathcal{B} \equiv \frac{Q}{\varepsilon_x \varepsilon_y \varepsilon_z}, \quad (1)$$

wherein ε_u is the rms emittance in the (u, p_u) -phase space: $\varepsilon_u \equiv [\langle u^2 \rangle \langle p_u^2 \rangle - \langle up_u \rangle^2]^{1/2}$ [(u, p_u) is the coordinate and associated canonical momentum], and Q the charge per bunch. The single-bunch brightness is situational: some applications such as high-average-current accelerators put stringent demands on the multi-bunch brightness (all the bunches within the bunch train should be aligned in the phase space), while other application such as single-pass FELs requires specific beam parameters over slices whose lengths are of the order of the so-called cooperation length, that is the slippage length between the radiation field and electron for one gain length. For an X-ray FEL (1 Å wavelength) these slices are typically $\sim 1 \mu\text{m}$ long.

PHOTOCATHODES AND ASSOCIATED DRIVE-LASER SYSTEMS

Given the quantum efficiency (QE) of the photocathode η , the drive-laser energy \mathcal{E} and wavelength λ , the charge of the photoemitted electron bunch is

$$Q = \eta \times \frac{e\lambda}{hc} \mathcal{E}, \quad \text{or} \quad Q[\text{nC}] \simeq \eta[\%] \times \frac{\lambda[\text{nm}]}{124} \mathcal{E}[\mu\text{J}], \quad (2)$$

assuming a single-photon emission process.

Metallic photocathodes are a popular choice for single-shot linacs. They require a UV drive laser and can be operated in modest vacuum conditions ($\sim 10^{-6}$ Torr). Copper cathodes especially have been widely used despite their poor QE ($\eta = 10^{-5}$), but are now being replaced by magnesium photocathodes having a higher QE ($\eta = 10^{-4}$).

Recent work on photo-thermal cathodes has been reported in Ref. [2, 3]. A typical photo-thermal cathode consists of a standard barium-impregnated tungsten cathode with an osmium surface coating. An alloy heater wire, buried behind the cathode, can increase the temperature of the cathode and thereby enhance the photoemission. These photocathodes have recently been tested in a rf gun and demonstrated QE values of $\simeq 10^{-4}$ [3].

Niobium has also been considered as a photoemitter: it is a natural choice envisioned for use in all-niobium superconducting rf (srf) guns [4]. However, niobium has a poor

*Work supported by Universities Research Association Inc. under Contract No. DEAC02-76CH00300 with the U.S. Department of Energy and by the Northern Illinois Center for Accelerator and Detector Development (NICADD).

QE ($\eta \simeq 10^{-5}$) when illuminated with UV (266 nm) and would require a high average laser power to be used for high-average-current accelerators. To circumvent this limitation, lead deposited on the niobium has been proposed as an alternative photocathode [5]. Lead is a good alternate photoemitter over a large range of UV wavelengths $\lambda \in [190 - 316]$ nm. Among various deposition mechanisms it has experimentally been shown that arc-deposited lead provides QEs close to 0.3% at 213 nm [5].

Semiconductor cathodes such as alkali tellurides have demonstrated high quantum efficiency (typically 1%) when illuminated with a UV laser and require vacuum levels easily achievable in photoinjectors. There are commonly used in rf-gun-based electron sources for FELs [6, 7]. Semiconductor cathodes such as CsKBr have much higher quantum efficiencies and operate well at green wavelengths, but are more sensitive to vacuum conditions.

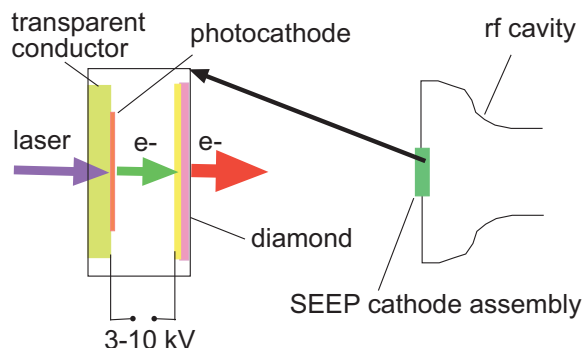


Figure 1: Schematics of a secondary-emission-enhanced photocathode (SEEP); see text for details. (Picture adapted from John Smedley of BNL)

Spin-polarized electron beams are produced using negative-electron-affinity (NEA) GaAs photocathodes. Strained GaAs/GaAsP superlattice photocathodes, consisting of very thin GaAs quantum well layers alternating with GaAsP barrier layers, have emerged as primary candidates [8]. The achieved polarization in superlattice photocathodes is greater than 85%¹, and quantum efficiencies of about 1% have been reported. To date NEA GaAs photocathodes have been operated in dc guns, and attempts to operate them in a rf gun have failed [9], the main challenge being to sustain the very demanding vacuum (10^{-11} Torr) during operation of the rf gun. Srf guns might be the natural candidates for operating GaAs cathodes, but other avenues are presently being explored (see next Section).

For future applications, such as ampère-class energy-recovering linear (ERL) accelerators, the use of metal cathodes would require MW-class photocathode-drive lasers. The secondary-emission-enhanced photocathode (SEEP) was proposed [10] to address this problem. A SEEP cathode assembly consists of a photocathode, a small gap, and a

diamond amplifier surface; see Fig. 1. Electrons are emitted from the photocathode and are accelerated across the vacuum gap with a dc voltage. When these “primary” electrons impact the diamond, they generate many secondary electrons which are ejected out of the diamond by an externally applied rf field. The SEEP cathode therefore increases the effective quantum efficiency by the ratio of secondary electrons generated per primary electron. Another benefit of SEEP is the thermalization of secondary electrons during their transport through the diamond, leading to a very low intrinsic emittance. Significant progress has been made on the development of the SEEP cathode. The latest results [11] demonstrated secondary electron generation, transport through a diamond plate, and ejection into vacuum in dc test beds. Progress has also been made on the design and fabrication of an encapsulated cathode for use in srf guns.

The photocathode-drive laser sets the initial conditions and, in turn, the electron-beam parameters depend on the laser performance. Tailoring the laser distribution in a predefined way such to linearize the space-charge forces is perceived as a next step for improving the beam brightness; see Fig. 2. To this end a desirable distribution is a cylinder with uniform charge distribution. Generating such a distribution has proven to be quite problematic in practice, mostly in the longitudinal plane. Techniques such as spectral shaping have tended to work in the fundamental mode of the laser system to yield reasonably uniform longitudinal distributions. However popular metal and some semiconductor photocathodes require UV light generated by frequency multiplication. This needed frequency up-conversion process often significantly degrades the laser pulse distribution both transversely and longitudinally. An alternate approach is directly to temporally stack Gaussian UV pulses to form the desired flat-top profile; complications include the need for alternate polarization of the stacked pulses to reduce interference effects [12]. The transverse uniformity can be controlled, even after frequency up-conversion, thanks to homogenization techniques using microlens arrays [13].

The ideal distribution is the 3D ellipsoid since the corresponding space-charge field is linear ($E_r \propto r$ and $E_z \propto z$). The production of such a distribution is challenging, and a technique initially proposed in Ref. [14] to operate in the so-called “blow-out” regime was recently studied in detail in Ref. [15]. It was shown that an ultrashort laser pulse, with proper transverse distribution, impinging upon a fast-response photocathode could produce a bunch that eventually equilibrates to a 3D ellipsoid. In practice, e.g. in a rf gun, there are still significant deteriorations of the ellipsoidal character of the distribution due to image charges, for instance. This “self-generating” method can easily be implemented, and preliminary experiments are encouraging [16]. A disadvantage of the self-generating method to produce a 3D ellipsoid is the lack of control over the bunch length. To address this feature it was suggested to use a 3D-ellipsoid-shaped photocathode-drive laser [17]. This

¹Other superlattices, such as InAlGaAs/GaAsP, have demonstrated peak polarization of 92%.

type of pulse shaping is efficient as long as the time scale of the required distribution is larger than the photoemission response time. Several techniques have been proposed to obtain a 3D-ellipsoid laser pulse. Spectral shaping is, in principle, the most straightforward. A temporal pulse stacker that stacks Gaussian pulses with different intensities and transverse sizes is also a potential candidate [17]. The use of silica fiber bundle and deformable mirrors is being investigated as possible shapers [18]. Finally the use of Fresnel (or zoned) lenses has been studied via numerical simulations and shown to be suitable for producing 3D ellipsoids with a proper shaping of each zone (shape, thickness, and transmission) of the lens [19].

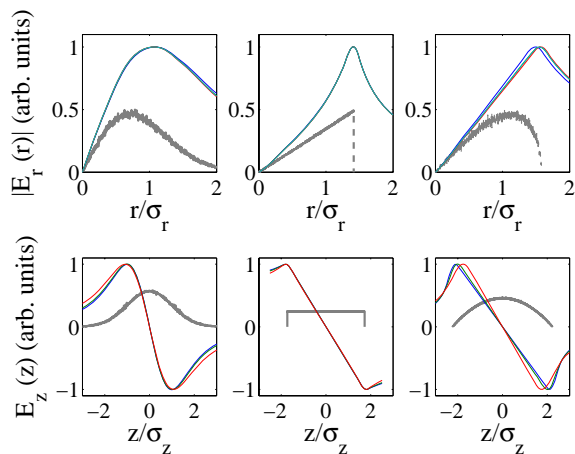


Figure 2: Transverse (top) and longitudinal (bottom) electric fields associated with a 3D Gaussian (left), a uniform cylinder with $\sigma_r/(\gamma\sigma_z) \simeq 10$ (middle), and a 3D ellipsoid (right) distribution. Color solid lines represent the field, while gray dashed lines correspond to the radial (top) and longitudinal (bottom) densities.

Specific applications such as high-average-current ERLs generally require high-average-power photocathode-drive lasers, and they can be challenging to build. In most critical cases of high-average-power FELs, it has actually been proposed to feed back a fraction of the light produced by the FEL to the photocathode [20]. Even the modest duty cycle associated with the International Linear Collider puts stringent demands on solid-state tunable² photocathode-drive lasers: high-average-power pumping diode arrays are not commercially available.

ACCELERATION FROM REST

The electron bunches emitted from the photocathode are accelerated as quickly as possible either in a dc gun or rf gun. The guns also often incorporate focusing element(s) to contain the generally highly divergent beams.

The dc guns are presently the only operating CW sources being used in high-average-current accelerators, e.g. Jeffer-

²The laser needs to have a tunable wavelength within range [700, 850] nm to allow matching to the cathode-proper transition.

son Lab's FELs [21]. Their main limitation is field emission. Significant progress has been made in reducing field emission by coating the electrodes with dielectric materials. Next-generation dc guns should be capable of operating with peak electric field as high as 25 MV/m. Transverse focusing can be provided by solenoids [22] or cathode shaping [23]. Because of the relatively low accelerating field, the production of high charge (few nC) generally requires an initial long laser pulse, and the resulting electron bunch needs to be longitudinally compressed with a bunching system [that usually incorporate sub-harmonic buncher(s)]. The main advantage of dc guns is the ability to sustain high vacuum quality compatible with the operation of NEA GaAs photocathodes. To date, polarized sources [24, 25] are exclusively based on dc guns.

Normal-conducting rf guns have been operated over a wide range of rf frequencies; see Ref. [26]. They have been systematically improved to ameliorate single-bunch beam parameters. The use of symmetrized rf-feed [27] or coaxial rf-input couplers [28] is now implemented in most designs to avoid emittance dilution due to a time-dependent dipole-like kick. Another contemplated improvement is the use of two-frequency rf-guns initially suggested in Ref. [29] to minimize the rf-induced emittance. A cavity capable of supporting two modes operating at 1.3 and 3.9 GHz has been designed [30], and beam-dynamics simulations performed for the Linac Coherent Light Source (LCLS) showed substantial improvement of the emittances compared to traditional single-frequency rf guns [31].

High-order-mode (HOM) rf guns, operating with the TM_{020} mode, have been proposed in Ref. [32]. A single HOM rf cavity is used to generate the desired on-axis axial E-field. The simulated beam properties are very similar to those obtained with traditional TM_{010} -mode cavities. This alternative design has the advantages of much greater ease of fabrication, immunity from coupled-cell effects, and simpler tuning procedures. Because of the gun geometry, the possibility also exists for improved temperature stabilization and cooling for high-duty-cycle applications. Finally, such a cavity is well suited for maintaining high-quality vacuum. The major disadvantage is low shunt impedance compared to traditional guns.

The Plane-Wave Transformer (PWT) structure is also a potential candidate to operate GaAs photocathodes. This is an open structure consisting of disks suspended from four water-carrying rods and mounted inside a large cylindrical tank. The rf power couples first into the annular region of the tank in a TEM-like mode, then couples into the accelerating cells in a TM-like mode [33]. The separation of the tank from the disks improves the conductance for vacuum pumping. According to beam-dynamics simulations, the PWT can operate at low gradient without significant degradation of beam quality, and this is beneficial for reducing ion back-bombardment on the photocathode.

The highest duty cycle rf gun operated to date was at the now-decommissioned Boeing FEL facility [34]. Progress to develop high-duty cycle rf-guns is being made [36]. A

CW L-band (750 MHz) rf gun, capable of peak E-field of 20 MV/m on the photocathode, has been designed for the LUX proposal. It uses a re-entrant shape cavity [35] and includes a coaxial rf input coupler located on the photocathode side, and a reversed dc-biased voltage in order to repel ions.

Srf guns are the most promising and yet most challenging-to-operate electron sources. If successful they could provide both the high average current presently achieved in dc guns along with single-bunch parameters similar to state-of-the-art rf guns. The design and first operation of a prototype L-band (1.3 GHz) srf gun (only 1/2-cell) was described in Ref. [37]. The srf gun must be installed in a cryogenic vessel and sustain a magnetic field, e.g., that of a solenoidal focusing lens. This field must not penetrate the superconducting cavity so as to avoid thermal breakdown. In this prototype design, focusing was provided by shaping the 1/2-cell back plate. This type of focusing is optimized for well-defined initial conditions (e.g. charge) and does not offer great flexibility. An alternative arrangement was studied in Ref. [38]: a solenoid lens is located downstream of a 1+1/2 cell 1.3 GHz srf gun resulting in a residual fringing field at the cavity location of a few gauss. The focusing is applied only after cool-down of the srf gun, and the small field is excluded from the superconducting cavity through the Meissner effect. It was shown that such a configuration can be optimized to obtain performance similar to photoinjectors based on normal-conducting rf guns. A peak E-field of 70MV/m is possible in srf guns with proper cell shaping [39]. Another proposed scheme for controlling the beam's transverse size is the use of TE-mode fields. In ref. [40], an L-band 3+1/2 cell rf gun was designed with its last cell also excited with a TE₀₂₁ mode. This mode provides a time-dependent axial magnetic field operating at a frequency close to 3.9 GHz. Optimization of this configuration demonstrated the usefulness of the TE mode to minimize the transverse emittance without major complication of the system.

In a rf gun, a focusing force can be provided at the photocathode surface by recessing the photocathode. This, however, is done at the expense of the peak E-field on the photocathode. A possible approach to focus the beam using electromagnetic forces is the planar-focusing cathode which allows independent tuning of the radial focusing and peak field on the cathode [41]. The scheme uses a dielectric cathode and include a shunt cylinder located behind the cathode. The beam is given a radial focusing kick as it leaves the cathode surface. The focusing strength, proportional to dE_z/dz can be varied independently of the gun gradient by adjusting the position of the shunt cylinder behind the cathode.

PHASE-SPACE MANIPULATIONS

It is common in accelerators to manipulate the phase space: the emittance compensation scheme [42, 43] or longitudinal bunch compression in a magnetic chicane exem-

plify such manipulations within one degree of freedom.

Recently schemes capable of manipulating the beam in two degree-of-freedom have emerged. An example is the round-to-flat transformation first proposed in Ref. [44] and later adapted to produce flat beams (i.e. beams with large transverse emittance ratio) directly out of a photoinjector. The beam is initially angular-momentum-dominated, with the angular momentum applied by immersing the photocathode in an axial magnetic field [45, 46]. A series of skew quads then removes the angular momentum, yielding the flat beam. An experimental study demonstrated a transverse emittance ratio of ~ 100 and verified most of the expected scaling laws inherent to the process [47, 48]. This flat-beam-production technique is attractive for the International Linear Collider since it may circumvent the need for an electron damping ring. However the main challenge is also to achieve, for the nominal charge of $Q = 3.2$ nC, a 4D emittance³ $\varepsilon_{4D} = \gamma[\varepsilon_x\varepsilon_y]^{1/2} \sim 0.4$ μm along with an emittance ratio of ~ 300 . The required value for the 4D emittance is one order of magnitude lower than what present state-of-the-art electron sources can reliably achieve.

Another example of phase-space manipulation aimed at exchanging coordinates within two degrees of freedom is the longitudinal-to-transverse emittance exchanger [49]. This exchanger consists of four bends arranged as a chicane in the horizontal plane (or a double-dogleg [50]) with a horizontally deflecting cavity (operating on the TM₁₁₀ mode) located in its center. Under proper choice of dispersion and deflecting voltage, the system has a 4×4 transfer matrix in (x, x', z, δ) that is antidiagonal and consists of 2×2 block matrices – such a transfer matrix clearly exchanges the transverse horizontal ε_x with the longitudinal emittance ε_z .

A linac concept that uses both the round-to-flat beam transformation and transverse-to-longitudinal emittance exchange was proposed for the “Greenfield” free-electron laser [51]. A low-charge (20 pC) bunch is generated in a photoinjector and optimized to produce low longitudinal and transverse normalized emittances $\gamma(\varepsilon_x, \varepsilon_y, \varepsilon_z) \rightarrow (4.7, 4.7, 0.08)$ μm with $\gamma\varepsilon_{4d} = 0.23$ μm . This angular-momentum-dominated beam is then accelerated and transformed into a flat beam thereby modifying the emittance partition to $\gamma(\varepsilon_x, \varepsilon_y, \varepsilon_z) \rightarrow (9.9, 0.005, 0.08)$ μm . Finally the horizontal and longitudinal emittances are exchanged and the final emittance partition $\gamma(\varepsilon_x, \varepsilon_y, \varepsilon_z) \rightarrow (0.08, 0.005, 9.9)$ μm . Although this is not an optimum operating point (it is preferable to have equal final transverse emittances), the achieved beam emittances have advantages: the large longitudinal emittance makes the beam less prone to space-charge-induced microbunching instabilities [52], while the low transverse emittances significantly reduces the FEL gain length. The same scheme might actually be applicable to the International Linear Collider.

³The 4D emittance is defined as the square root of the determinant of the beam matrix in (x, x', y, y') phase space

MODELING

Although analytical modeling of photoinjectors is intricate, and the simple theory of emittance compensation proposed in Ref. [42] was later refined in Ref. [43], recent promising work based on a Hamiltonian treatment has been reported [53]. From a linear Hamiltonian, the beam-envelope evolution is obtained, and it gives a better physical picture of the emittance-compensation process compared to previous theory. This recent theoretical work is also able to reproduce most of the features observed in numerical simulations, especially the double emittance minima.

Particle-in-cell simulation programs based on the electrostatic approach are still widely used and subject to constant improvements. Astra [54] and Impact-T [55] incorporate a quasistatic approach that takes into account energy spread (and therefore relative motion in the rest frame). A recent improvement of Impact-T incorporates a wavelet-based space-charge algorithm [56]. Wavelet decomposition of the phase-space density allows denoising (that can reduce the needed number of macroparticle) and provides a way to store the phase-space distribution compactly. This can be useful for halo studies and simulating how coherent synchrotron radiation affects the beam dynamics (since integration over the retarded potential is required). Finally a fully self-consistent program, VORPAL 2.0, has been efficiently parallelized, providing a powerful numerical tool for detailed beam-dynamics investigations [57].

ACKNOWLEDGMENTS

I would like to thank M. Ferrario (INFN Frascati), K. Flöttmann (DESY), and J. Lewellen (ANL) for enlightening discussions on photoinjectors over the past years. This paper has benefited from talks given by participants of Working Group 5 at the Advanced Accelerator Concepts Workshop (AAC'06). I finally would like to thank C.L. Bohn (Northern Illinois University) and Y.-E Sun (ANL) for comments on the manuscript.

REFERENCES

[1] M. Ferrario, PAC 2005, p. 530 (2005).
 [2] D. W. Feldman *et al.*, PAC 2001, p. 2132 (2001).
 [3] Y.-E Sun and J.W. Lewellen, these proceedings.
 [4] T. Rao *et al.*, PAC 2005, p. 2556 (2005).
 [5] J. Smedley, *et al.*, PAC 2005, p. 2598 (2005).
 [6] D. Sertore, *et al.*, PAC 2005, p. 671 (2005).
 [7] S.H. Kong, *et al.*, NIM A **358**, p. 272 (1995).
 [8] T. Maruyama *et al.* APL, **85**, p. 2640 (2004).
 [9] A. V. Aleksandrov, *et al.*, EPAC 1998, p. 1450 (1998).
 [10] X. Chang, *et al.*, PAC 2005, p. 2251 (2005).
 [11] J. Smedley, *et al.*, presented at the Advanced Accelerator Concept Workshop (AAC06), Lake Geneva WI July 2006.
 [12] J. Li, *et al.*, NIM A **564**, p. 57 (2006).

[13] H. Tomizawa, *et al.*, EPAC 2002, p. 1819 (2002).
 [14] L. Serafini, AIP Conf. Proc. **413**, p. 321 (1997).
 [15] O. J. Luiten *et al.*, PRL **93**, 094802 (2004).
 [16] J. Rosenzweig, *et al.*, presented at the AAC06; see ref. [11].
 [17] C. Limborg-Deprey, *et al.*, NIM A **557**, p. 106 (2006).
 [18] H. Tomizawa, *et al.*, NIM A **557**, p. 117 (2006).
 [19] Y. Li, *et al.*, these proceedings.
 [20] K.-J. Kim *et al.*, NIM A **405**, p. 380 (1998).
 [21] G. R. Neil, *et al.*, PRL **84**, p. 662 (2000).
 [22] D. Engwall, *et al.*, PAC 1997, p. 909 (1998).
 [23] I Bazarov and C. K. Sinclair, PRSTAB **8**, 034202 (2005).
 [24] C. K. Sinclair, PAC 1999, p. 65 (1999).
 [25] A. Brachmann *et al.*, PAC 2005, p. 3420 (2005).
 [26] for a review see P. Piot, DESY-report M 02-02 (2002).
 [27] L. Xiao, *et al.*, PAC 2005, p. 3432 (2005).
 [28] D. Dwersteg *et al.*, NIM A **393**, p. 93 (1997).
 [29] L. Serafini, NIM A **318**, p. 301 (1992).
 [30] J.W. Lewellen, and J. Noonan, PRSTAB **8**, 033502 (2005).
 [31] D. H. Dowell *et al.*, NIM A **528**, p. 316 (2004).
 [32] J.W. Lewellen, *et al.*, PRSTAB **4**, 040101 (2001).
 [33] D. Yu, *et al.* these proceedings.
 [34] D. Dowell *et al.*, APL **63** (15), p. 167 (1993).
 [35] R. A. Rimmer, PAC 2005, p. 3049 (2005).
 [36] A.M.M. Todd, *et al.*, PAC 2005, p. 2292 (2005).
 [37] D. Janssen, *et al.*, NIM A **452**, p. 34 (2000).
 [38] M. Ferrario, *et al.*, NIM A **557**, p. 98 (2006).
 [39] J. Seckutowicz, these proceedings.
 [40] D. Janssen, *et al.*, PRSTAB **7**, 090702 (2004).
 [41] J. W. Lewellen, PAC 2005, p. 563 (2005).
 [42] B.E. Carlsten, NIM A **250**, 313 (1989).
 [43] L. Serafini, and J. Rosenzweig PRE **55**, 7565 (1995).
 [44] Ya. Derbenev, University of Michigan Report No. UM-HE-98-04 (1998).
 [45] R. Brinkmann, *et al.*, PRSTAB **4**, 053501 (2001).
 [46] K.-J. Kim, PRSTAB **6**, 104002 (2003).
 [47] Y.-E Sun, PhD Thesis University of Chicago (2005), also report Fermilab-thesis-2005-17 (2005).
 [48] P. Piot, *et al.*, PRSTAB **9**, 031001 (2006).
 [49] M. Cornacchia and P. Emma, PRSTAB **5**, , 084001 (2002).
 [50] K.-J. Kim and A. Sessler, AIP Conf. Proc. **821**, p. 115 (2006).
 [51] P. Emma, *et al.*, preprint FERMILAB-PUB-06-256-AD/SLAC PUB 1000-86 (2006).
 [52] Z. Huang and K.-J. Kim, PRSTAB **5**, 074401 (2002).
 [53] C.X. Wang, PAC 2005, p. 1476 (2005).
 [54] K. Flöttmann, "ASTRA: A Space Charge Tracking Algorithm", available at <http://www.desy.de/~mpyf1o>.
 [55] J. Qiang, *et al.*, PRSTAB **9**, 044204 (2006).
 [56] B. Terzic, *et al.*, PAC 2005, p. 2601 (2005).
 [57] C. Nieter and J. R. Cary, J. of Comp. Phys. **196** (2), 448 (2004).